Journal of Clinical and Translational Hepatology **2026**
DOI: 10.14218/JCTH.2026.00215

Original Article

Palmatine Induces TNNT1 Ubiquitination and Degradation to Potentiate Ferroptosis Sensitivity in Hepatocellular Carcinoma

Xiaokang Wang[1], Fanci Xie[2], Chunhua Wang[3], Shangjun Zhou[4], Jiayu Wang[4], Zhijie Xu[4] and Zhiyang Zhou[5,6*]

[1]Department of Pharmacy, Shenzhen Longhua District Central Hospital, the Affiliated Longhua Hospital of Shenzhen University, Shenzhen, Guangdong, China; [2]Department of Hepatology, The Fourth Clinical Medical College of Guangzhou University of Chinese Medicine, Guangzhou, Guangdong, China; [3]Department of Oral Bioscience, Tokushima University Graduate School of Biomedical Sciences, Tokushima, Japan; [4]Department of Pathology, Xiangya Hospital, Central South University, Changsha, Hunan, China; [5]Department of Breast Surgery, National Clinical Research Center for Geriatric Disorders, Xiangya Hospital, Central South University, Changsha, Hunan, China; [6]Clinical Research Center for Breast Cancer in Hunan Province, Changsha, Hunan, China

Received: March 27, 2026 | **Revised:** May 14, 2026 | **Accepted:** July 20, 2026 | **Published online:** August 19, 2026

Abstract

Background and Aims: Ferroptosis, an iron-dependent form of regulated cell death, serves as an important mechanism associated with cancer progression. Natural compounds, particularly alkaloids, have emerged as attractive candidates for regulating ferroptotic cell death, thereby providing a promising anticancer strategy. However, the molecular mechanisms underlying their antitumor effects remain poorly understood. In this study, we aimed to investigate the antitumor effects and underlying mechanisms of natural alkaloids against HCC. ***Methods:*** An alkaloid library was used to screen alkaloids with anti-hepatocellular carcinoma (HCC) activity. A combination of proteomic profiling, *in vitro* functional assays, and *in vivo* animal experiments was performed to explore the biological roles and molecular mechanisms of the lead compound. ***Results:*** Through high-throughput screening of an alkaloid library, we identified palmatine (PAL), an active component isolated from *Fibraurea recisa* Pierre, as a potential ferroptosis sensitizer in HCC cells. PAL treatment triggered typical ferroptotic features in HCC cells, including elevated ferrous iron, reactive oxygen species, and lipid peroxidation, along with decreased glutathione levels. Importantly, the pro-ferroptotic effect of PAL was significantly abolished by two ferroptosis inhibitors, ferrostatin-1 and deferoxamine. Mechanistically, PAL directly interacted with troponin T1 (TNNT1) to trigger its K48-linked polyubiquitination and subsequent protein degradation. Ectopic TNNT1 overexpression significantly rescued PAL-mediated ferroptosis and abrogated its tumor-suppressive effects. *In vivo* animal models further confirmed that PAL suppressed tumor growth by downregulating TNNT1, with a favorable safety profile. ***Conclusions:*** Therefore, this study reveals a previously unrecognized role of PAL as a ferroptosis sensitizer and highlights its translational potential for anti-HCC therapy.

Citation of this article: Wang X, Xie F, Wang C, Zhou S, Wang J, Xu Z, *et al*. Palmatine Induces TNNT1 Ubiquitination and Degradation to Potentiate Ferroptosis Sensitivity in Hepatocellular Carcinoma. J Clin Transl Hepatol 2026. doi: 10.14218/JCTH.2026.00215.

Introduction

Hepatocellular carcinoma (HCC), the most common histological subtype of primary liver cancer,[1] is a leading cause of cancer-associated mortality worldwide.[2] Over the past few decades, its global incidence and mortality have risen consistently, presenting an increasingly severe threat to public health.[3] HCC tumorigenesis is a complex, multistep process driven by a diverse array of risk factors, including chronic viral hepatitis infection, metabolic syndrome, and inherited hepatic disorders, etc.[4,5] Despite notable advances in clinical management strategies, such as surgical resection, liver transplantation, and systemic therapies (tyrosine kinase inhibitors and immune checkpoint inhibitors), the clinical prognosis of HCC patients remains poor.[6,7] Most HCC patients are diagnosed at advanced and unresectable stages, largely owing to the lack of sensitive and specific biomarkers for early detection.[8] In addition, high rates of postoperative recurrence, distant metastasis, and acquired drug resistance greatly limit the efficacy of existing therapeutic strategies.[9,10] These intractable clinical challenges are tightly associated with the intricate molecular and cellular mechanisms underlying HCC initiation, progression, and therapeutic resistance, which remain largely elusive to date. HCC is hallmarked by the dysregulation of multiple tumor-associated signaling pathways, which dynamically orchestrate tumorigenesis and therapeutic evasion.[11,12] Thus, there is an urgent and unmet clinical need to unravel novel cellular and molecular

Keywords: Hepatocellular carcinoma; Natural alkaloids; Palmatine; TNNT1 ubiquitination; K48-linked polyubiquitination; Ferroptosis.

***Correspondence to:** Zhiyang Zhou, Department of Breast Surgery, National Clinical Research Center for Geriatric Disorders, Xiangya Hospital, Central South University, Changsha, Hunan 410008, China. ORCID: https://orcid.org/0009-0007-8320-9385. Tel: +86-15388011095, Fax: +86-73189753015, E-mail: zzywy00000@163.com or zhouzy@csu.edu.cn.

mechanisms governing HCC development and progression. Elucidating these fundamental mechanisms is critical to filling key knowledge gaps in HCC biology, which will ultimately facilitate improvements in long-term survival outcomes for HCC patients worldwide.

Ferroptosis is an iron-dependent, lipid peroxidation-mediated form of regulated cell death. It differs from other cell death types, mainly due to its characterization by cellular redox imbalance and glutathione peroxidase 4 (GPX4) dysfunction.[13–15] As a critical biological process in cancer, including HCC, ferroptosis is frequently dysregulated in malignant cells, which evolve robust evasion mechanisms to escape ferroptotic cell death—an adaptive trait that drives tumor progression, metastasis, and resistance to conventional anticancer therapies.[16–18] Chen's group used integrated multi-omics technologies and found that tumor cells within the primary lesion exhibited both epithelial–mesenchymal transition and ferroptosis-associated signatures, which contribute to the formation of portal vein tumor thrombus in HCC.[19] Increased SCRN1 expression in HCC cells significantly impaired autophagy-mediated degradation of GPX4 by enhancing its phosphorylation, consequently alleviating lipid peroxidation and conferring ferroptosis resistance.[20] Sor@Fe-MOF nanoparticles could drive ferroptotic cell death through downregulating GPX4 and upregulating ACSL4, exhibiting favorable therapeutic activity against HCC.[21] Thus, elucidating the precise molecular networks governing ferroptosis in cancer cells holds great promise for developing novel, precision-based ferroptosis-inducing therapeutic strategies for HCC treatment.

Natural products represent a promising source for innovative drug discovery and are highly valued for their significant biomedical applications.[22,23] As an important class of natural products, alkaloids possess attractive antitumor pharmacological properties.[24] For example, a natural alkaloid isolated from *Fibraurea recisa* Pierre, named palmatine (PAL), possesses a wide spectrum of pharmacological bioactivities, such as anti-inflammatory[25] and antitumor effects.[26] Administration of PAL obviously induced G2/M-phase arrest and antagonized the malignant phenotype of colorectal cancer cells by inhibiting myosin heavy chain 9-mediated nuclear localization of aurora kinase A.[27] Another study by Ativui's group indicated that PAL displayed an obvious cytotoxic effect through inhibition of metastasis in 4T1 triple-negative breast cancer cells.[28] Although PAL has shown potential for HCC therapy,[29] its detailed molecular mechanisms have not been fully elucidated.

The present study aimed to investigate the antitumor effects and underlying mechanisms of natural alkaloids against HCC. Using high-throughput screening (HTS) of an alkaloid library, we identified PAL as a potential anti-HCC agent. Our results demonstrated that PAL exerted potent antitumor activity by inducing ferroptosis both *in vitro* and *in vivo*. To explore the molecular mechanisms underlying PAL-mediated cytotoxicity, quantitative proteomics was performed to identify differentially expressed proteins (DEPs) in HCC cells following PAL treatment. We found that PAL markedly downregulated troponin T1 (TNNT1) expression by promoting its K48-linked polyubiquitination. Collectively, this study represents a proof of concept for a screening paradigm to develop PAL as a promising candidate for HCC treatment.

Methods

Cell culture and reagents

The HCC cell lines HepG2 and Huh7, as well as normal hepatic HHL5 cells, were all provided by Xiangya Cancer Center, Xiangya Hospital, Central South University, China. Cultured in Dulbecco's Modified Eagle's Medium (Corning) supplemented with 10% fetal bovine serum (Gibco) and 1% penicillin/streptomycin, these cells were grown in a humidified incubator at 37 °C with 5% CO_2.

The alkaloid library containing 269 compounds (L7900), PAL (S3769), and MG132 (S2619) were all acquired from Selleckchem. GPX4 antibody (67763-1-Ig) and 4-hydroxynonenal (4-HNE) antibody (68538-1-Ig) were acquired from Proteintech. TNNT1 antibody (NBP1-32748) was acquired from Novus Biologicals. Actin antibody (sc-58673) was acquired from Santa Cruz Biotechnology. Ubiquitin antibody (#3936) was acquired from Cell Signaling Technology.

Cell viability and growth assays

Cell viability was quantified using the Cell Counting Kit-8 (CCK-8, B34304, Bimake) assay following a previously described protocol.[23] A total of 2×10^3 HCC cells were inoculated into 96-well plates. Following cell adhesion, cells were treated with the indicated compounds for various durations. Subsequently, 10 μL of CCK-8 reagent was added to each well, followed by incubation for 2 h. The absorbance of the resulting complex was detected at 450 nm using a microplate reader. The cell inhibitory rate was calculated according to the following formula:

$$\text{Inhibition rate} = 1 - \frac{\text{OD\_compound} - \text{OD\_blank}}{\text{OD\_Ctrl} - \text{OD\_blank}}.$$

Cell growth was evaluated using the colony formation assay. As described previously,[30] 1×10^3 HCC cells were inoculated into 6-well plates. Following cell adhesion, cells were treated with the indicated compounds. After nearly 14 days of culture, HCC cells were washed with pre-cooled phosphate-buffered saline and fixed with pre-cooled methanol. Thereafter, 0.3% crystal violet solution was used to stain the cell colonies.

Cell death assay

Cell death was quantified using the Calcein/PI Live/Dead Viability/Cytotoxicity Assay Kit (C2015M, Beyotime) following a previously described protocol.[31] HCC cells were seeded onto glass coverslips. After treatment with the indicated compounds, the cells were stained with 1 mL of Calcein acetoxymethyl ester (AM)/propidium iodide (PI) solution at 37 °C for 30 min in the dark. A fluorescence microscope (ZEISS Axio Observer 3) was used to detect fluorescence staining of the cells. Specifically, green fluorescence from Calcein AM indicated living cells, while red fluorescence from PI indicated dead cells.

Intracellular Fe^{2+} analysis

Intracellular ferrous iron (Fe^{2+}) levels were quantified using an iron assay kit (labscience, E-BC-K881-M) following a previously described protocol.[31] Cells were lysed on ice and centrifuged at 15,000 × *g* for 15 min. The supernatant was collected and incubated with the iron probe at 37 °C for 60 min in the dark. The absorbance of the generated complex was detected at 593 nm using a microplate reader. The Fe^{2+} concentration was then quantified based on the proportional relationship between absorbance intensity and Fe^{2+} content.

Intracellular malondialdehyde (MDA) assay

Intracellular MDA content was quantified using the Malondialdehyde ELISA Kit (MEIMIAN) following a previously described protocol.[31] A total of 1×10^6 HCC cells were homogenized on ice in butylated hydroxytoluene-containing MDA lysis buffer. After centrifugation at 13,000 × *g* for 10 min, the superna-

tant was collected and incubated with thiobarbituric acid solution at 95 °C for 1 h. The absorbance of the generated MDA-thiobarbituric acid adduct was detected at 532 nm. The MDA concentration was then quantified based on the proportional relationship between absorbance intensity and MDA content.

Reactive oxygen species (ROS) assay

The cellular ROS concentration was quantified using the DCFDA/H_2DCFDA Kit (35845, Sigma) following a previously described protocol.[31] After treatment with the indicated compounds, suspended HCC cells were stained with DCFDA solution for approximately 30 min in the dark. A fluorescence microscope (ZEISS Axio Observer 3) was used to detect cells with green fluorescence signals.

Western blot

Western blot analysis was performed following a previously described protocol.[31] Approximately 50 μg of proteins extracted from HCC cells or tumor tissues were separated by 10% sodium dodecyl-sulfate polyacrylamide gel electrophoresis and transferred onto methanol-activated polyvinylidene fluoride membranes by electroblotting. The membranes were then shaken in 5% defatted milk-containing Tris-buffered saline for 1 h, followed by incubation with the following primary antibodies: GPX4 antibody, TNNT1 antibody, 4-HNE antibody, ubiquitin antibody, and actin antibody.

HCC mouse model

Animal experiments were performed following a previously described protocol.[21] BALB/c nude mice (3–4 weeks old) were purchased from Sleck Jingda (Hunan, China). Approximately 5×10^6 Huh7 cells were subcutaneously injected into the flanks of mice to establish xenograft tumors. When the tumor volume reached approximately 100 mm^3, all mice were randomly divided into four groups: the Control (Ctrl) group, PAL-treated group, PAL + Flag-Ctrl group, and PAL + Flag-TNNT1 group. After a 20-day treatment cycle, all mice were euthanized. Tumor tissues, as well as major organs (heart, liver, spleen, lung, and kidney), were surgically excised and reserved for the indicated analyses. The Ethics Committee of Xiangya Hospital, Central South University, approved these animal experiments (XY20260303003).

Statistical analysis

All experimental findings are presented as mean ± standard deviation. Results represent at least three independent experiments. Two-tailed unpaired or paired Student's t-tests were used to calculate statistical significance between two groups. The relationship between two variables was analyzed using Pearson correlation coefficients. All statistical procedures were conducted using GraphPad Prism 8 software (San Diego, CA, USA), with significance thresholds set at $P < 0.05$ and $P < 0.01$.

Results

HTS methods identify PAL as the potential anti-HCC alkaloid

We screened a small alkaloid library to explore its inhibitory effects against HCC cells. A total of 269 alkaloid compounds were tested in Huh7 cells at a concentration of 10 μM, and the results are presented as the percentage of cell inhibition relative to untreated Ctrl cells. Among the 269 compounds examined, PAL exhibited the most potent inhibitory effect on tumor cell viability (Fig. 1A and B). We subsequently used the CCK-8 assay to confirm the antitumor effects of PAL in Huh7 and HepG2 cells. As expected, PAL effectively inhibited tumor cell survival in a time- and dose-dependent manner (Fig. 1C and D). In contrast, no significant effects of PAL were observed in normal hepatic HHL5 cells (Fig. 1E). Next, clonogenic survival assays were performed to investigate the role of PAL in regulating cell growth. As shown in Figure 1F, exposure of Huh7 and HepG2 cells to PAL led to a significant decrease in colony formation compared with that in Ctrl cells. Meanwhile, live/dead cell staining was performed to evaluate the extent of cell death. PAL treatment resulted in a higher proportion of PI-positive dead cells (Fig. 1G), suggesting that PAL was highly effective in promoting cell death in HCC cells. Based on these results, we selected PAL as a candidate anti-HCC drug for further mechanistic investigation.

PAL successfully exerted stimulatory effects on ferroptosis

Following confirmation of PAL's cytotoxicity against HCC cells, we conducted further research to determine how PAL affects cell death. To characterize the biological effects of PAL treatment on changes in the cellular proteome, Huh7 cells were treated with PAL or dimethyl sulfoxide. Subsequently, protein extracts were trypsinized and analyzed using quantitative proteomics. The DEPs were defined as $|\log_2(\text{fold change})| \geq 1$ (Supplementary Table 1). Functional enrichment analysis of these DEPs indicated that several ferroptosis-associated pathways, such as ROS metabolism, glutamate receptor activity, and adenosine triphosphate (ATP) metabolism, were overrepresented in PAL-treated Huh7 cells (Fig. 2A). Moreover, as depicted in Figure 2B, the inhibitory effect of PAL on cell viability was significantly abolished by two ferroptosis inhibitors, ferrostatin-1 and deferoxamine.[32] The elevated Fe^{2+}, ROS, and lipid peroxidation levels, accompanied by decreased reduced glutathione (GSH) levels, are typical hallmarks of ferroptosis.[33] Accordingly, the intracellular contents of Fe^{2+} and the lipid peroxidation product MDA were both significantly increased in PAL-treated Huh7 and HepG2 cells (Fig. 2C and D). In contrast, PAL treatment significantly reduced GSH levels in Huh7 and HepG2 cells (Fig. 2E). GPX4 expression, another key indicator of ferroptosis, effectively reflects the cellular ability to detoxify lipid peroxides.[34] Here, GPX4 expression was investigated by western blot, and as shown in Figure 2F, GPX4 expression was clearly downregulated in Huh7 and HepG2 cells treated with PAL. Given the critical physiological roles of ferroptosis in promoting the release of damage-associated molecular patterns (DAMPs), including ATP secretion and passive release of high mobility group protein B1 (HMGB1),[35] we sought to explore the regulatory effect of PAL on DAMP homeostasis. Upon PAL treatment, we observed increased extracellular levels of HMGB1 and ATP (Fig. 2G and H), confirming the stimulatory effect of PAL on DAMP release. Taken together, the above-mentioned results demonstrated that PAL induced ferroptotic cell death and represented a promising agent for the treatment of ferroptosis-related HCC.

Identification of proto-oncogenic TNNT1 as the potential target of PAL

To identify potential targets of PAL in HCC, we analyzed the DEPs in PAL-treated Huh7 cells. Heatmap analysis identified TNNT1 as the most significantly downregulated protein (Fig. 3A), suggesting that it may serve as a potential therapeutic target of PAL. Next, we determined the effect of PAL on TNNT1 expression in Huh7 and HepG2 cells by western blot and quantitative real-time polymerase chain reaction. Interestingly, the results demonstrated that PAL treatment down-

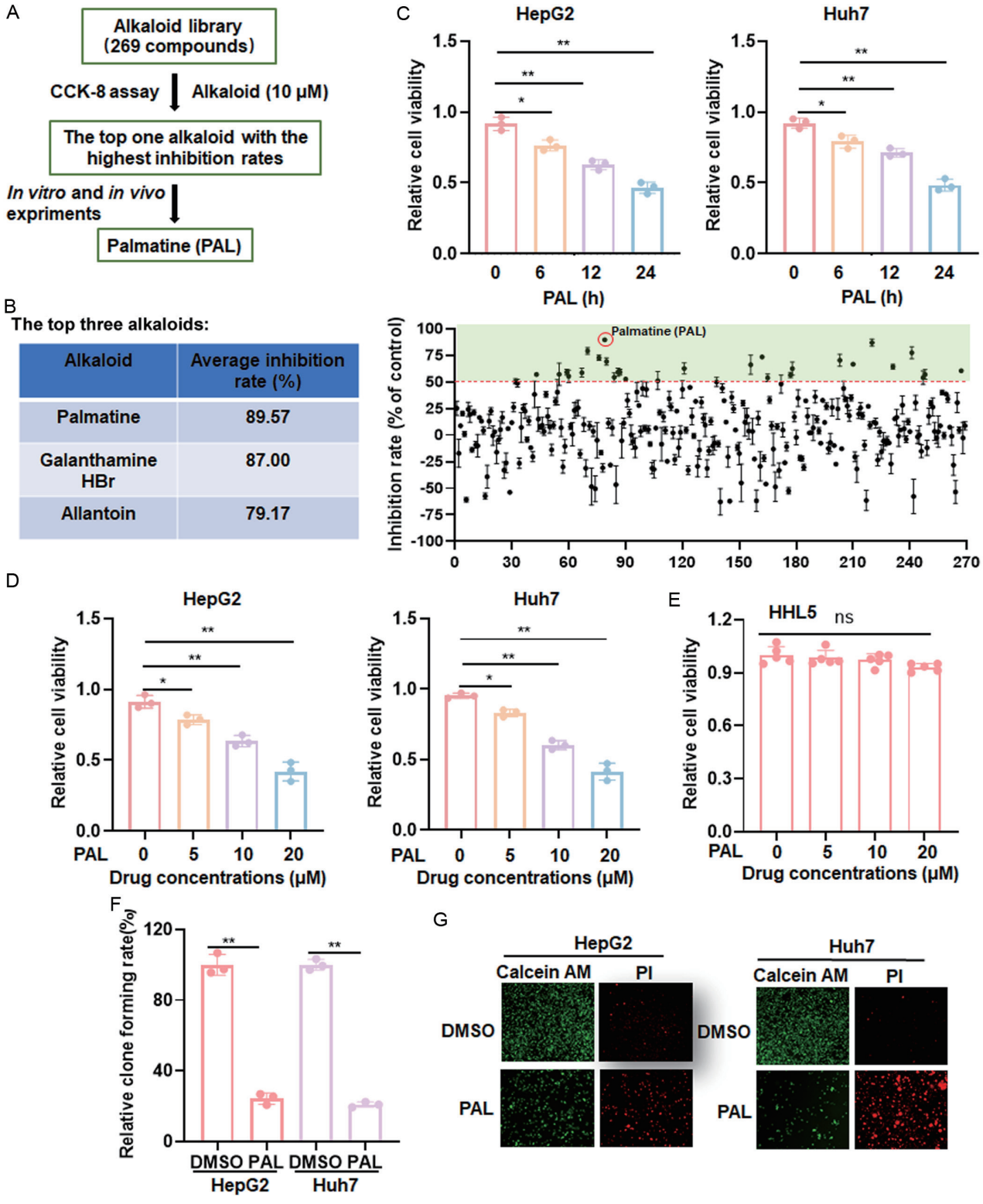

Fig. 1. Identification of PAL as an anti-HCC alkaloid. (A) Schematic workflow of alkaloid library screening for anticancer candidates. (B) The CCK-8 assay indicated the inhibitory effects of 269 alkaloid compounds on HCC cell viability. The top three candidate alkaloids with obvious anti-HCC activity were also displayed. (C-D) The time- and dose-dependent effects of PAL on HCC cells Huh7 and HepG2. (E) Changes in the viability of normal hepatic HHL5 cells after PAL treatment. (F) Clonogenic survival assays indicated the roles of PAL in regulating cell growth. (G) Live/dead cell staining indicated the roles of PAL in regulating cell death. Calcein AM (green) stained live cells, and PI (red) labeled dead cells. NS, not significant. *P < 0.05; **P < 0.01. HCC, hepatocellular carcinoma; CCK-8, Cell Counting Kit-8; PAL, palmatine; PI, propidium iodide; AM, acetoxymethyl ester; DMSO, dimethyl sulfoxide.

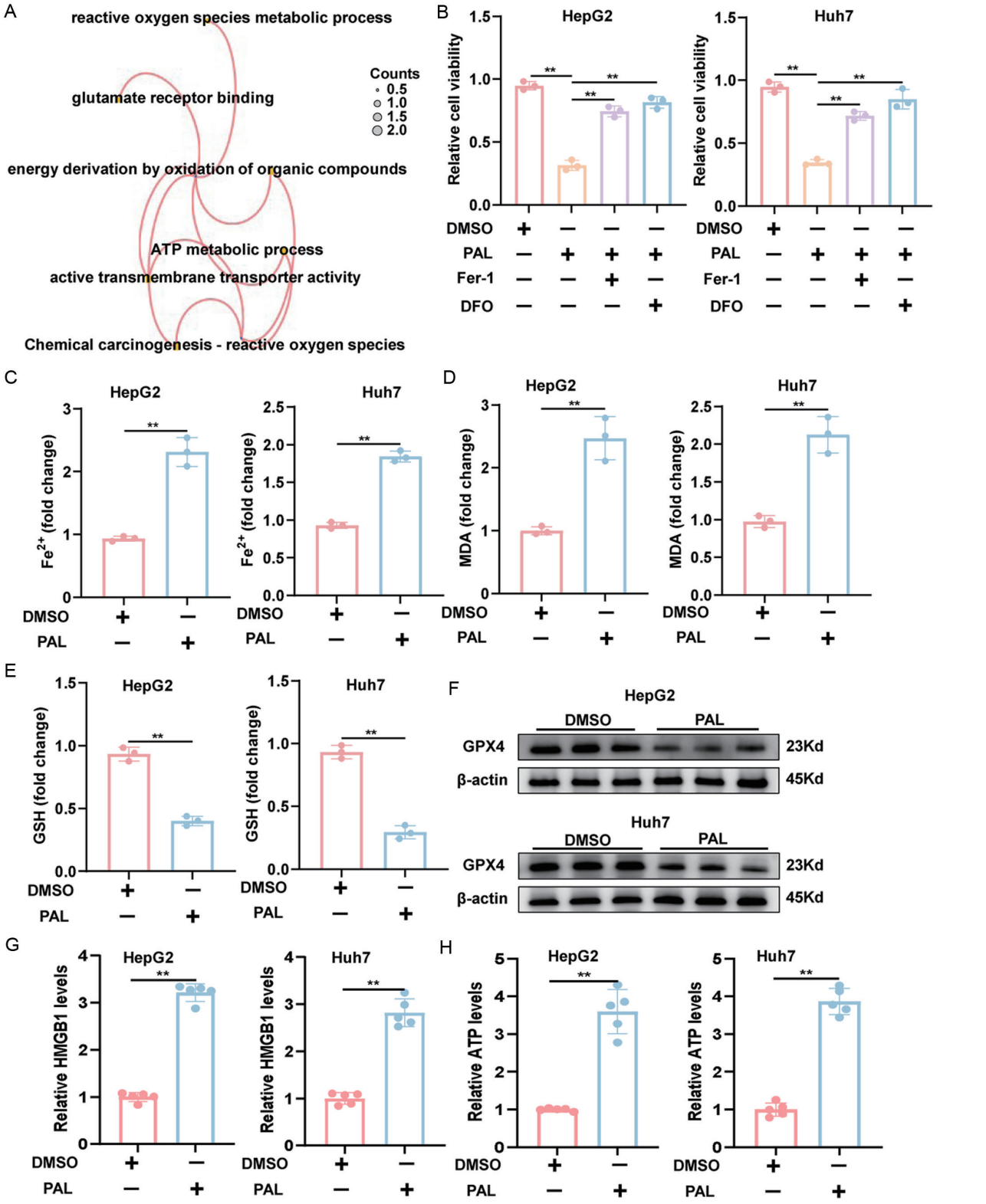

Fig. 2. PAL-induced effects on ferroptosis. (A) Functional enrichment analysis of the DEPs upon PAL exposure. (B) The regulatory effects of two ferroptosis inhibitors, Fer-1 and DFO, on PAL-mediated cell viability inhibition. (C) The effects of PAL on Fe^{2+} levels. (D) The effects of PAL on lipid peroxidation product MDA levels. (E) The effects of PAL on GSH levels. (F) The effects of PAL on the expression of the ferroptosis biomarker GPX4. (G-H) The effects of PAL on the release of HMGB1 and ATP. $^{**}P < 0.01$. DEPs, differentially expressed proteins; Fer-1, ferrostatin-1; DFO, deferoxamine; PAL, palmatine; Fe^{2+}, ferrous iron; MDA, malondialdehyde; DMSO, dimethyl sulfoxide; ATP, adenosine triphosphate; HMGB1, high mobility group protein B1; GSH, reduced glutathione; GPX4, glutathione peroxidase 4; +, with; -, without.

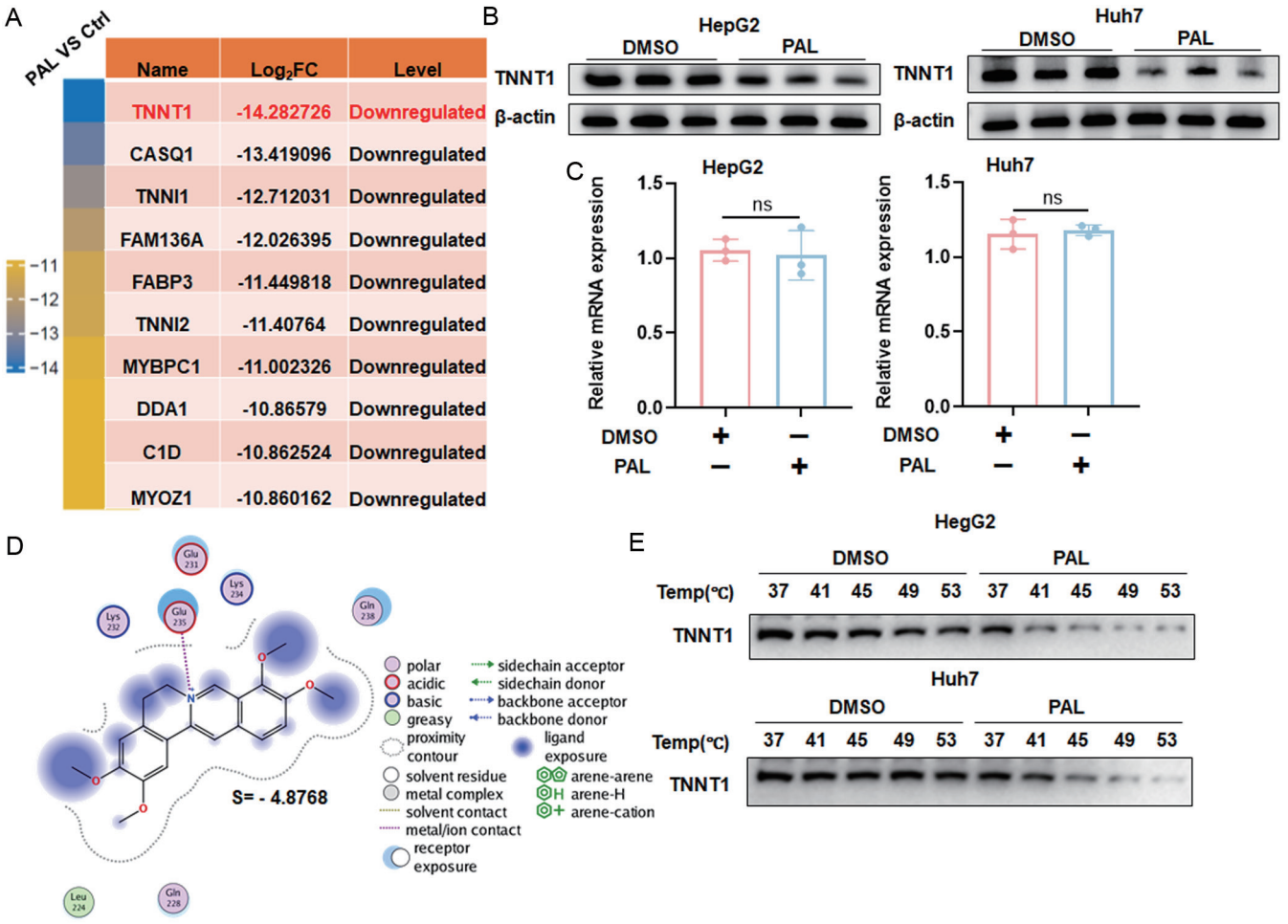

Fig. 3. Identification of TNNT1 as the potential target of PAL. (A) Heatmap of the significantly downregulated proteins. (B-C) The effects of PAL on the expression of TNNT1. (D) Molecular docking analysis of PAL and TNNT1. (E) CETSA analysis of the PAL-TNNT1 direct interaction in HCC cells. NS, not significant; PAL, palmatine; CETSA, cellular thermal shift assay; HCC, hepatocellular carcinoma; Log2 FC, Log2 fold change; TNNT1, troponin T1; CASQ1, calsequestrin 1; TNNI1, troponin I1; FAM136A, family with sequence similarity 136 member A; FABP3, fatty acid binding protein 3, TNNI2, troponin I2; MYBPC1, myosin binding protein C1; DDA1, DET1- and DDB1-associated 1; C1D, C1D nuclear receptor corepressor; MYOZ1, myozenin 1; DMSO, dimethyl sulfoxide; Ctrl, Control; +, with; -, without.

regulated TNNT1 at the protein level but exerted no effect on its mRNA transcription (Fig. 3B and C). We then employed Molecular Operating Environment software to perform molecular docking analysis between PAL and TNNT1. As shown in Figure 3D, PAL could be well docked into the TNNT1 protein structure, with a docking score of −4.8768. Accumulating studies have shown that the cellular thermal shift assay (CETSA) can be used to evaluate the direct interaction between drugs and endogenous targets in cells.[31,36] CETSA analysis revealed that PAL treatment significantly decreased the thermal stability of TNNT1 in HCC cells, supporting the direct binding of PAL to TNNT1 (Fig. 3E). As reported, TNNT1 might be a proto-oncogenic biomarker for several cancers, including HCC.[37] To evaluate changes in TNNT1 expression across pan-cancers, we analyzed high-throughput genomics data from human cancer patients using the HCC Database v2.0 platform.[38] TNNT1 expression was significantly upregulated in multiple cancers, including bladder urothelial carcinoma, breast cancer, lung adenocarcinoma, etc. (Supplementary Fig. 1A). Moreover, three HCC datasets all confirmed the upregulation of TNNT1 in HCC tissues (Supplementary Fig. 1B). We evaluated the prognostic value of TNNT1 in HCC patients using Kaplan-Meier Plotter,[39] and found that high TNNT1 expression was significantly associated with poor overall survival and recurrence-free survival (Supplementary Fig. 1C and D). Another two Gene Expression Omnibus datasets (GSE76427[40] and GSE10186[41]) from PanCanSurvPlot[42] also confirmed the unfavorable prognostic value of TNNT1 for patients' overall survival (Supplementary Fig. 1E and F). Taken together, these findings collectively suggested that PAL might inhibit the expression of the tumor promoter TNNT1 in human HCC cells.

PAL promoted TNNT1 K48-linked ubiquitination

Administration of PAL reduced TNNT1 protein levels but had no effect on its mRNA levels (Fig. 3B and C), indicating that PAL regulates TNNT1 at the post-translational level. Meanwhile, as shown in Fig. 4A, the PAL-induced decrease in TNNT1 protein levels was abolished by the proteasome inhibitor MG132,[43] suggesting that PAL modulates TNNT1 stability through the ubiquitin-proteasome pathway. Using cycloheximide chase assays, we further determined the protein stability of TNNT1. As expected, PAL treatment markedly shortened the protein half-life of TNNT1 in Huh7 and HepG2 cells (Fig. 4B). As K48-linked ubiquitination is critical for regulating

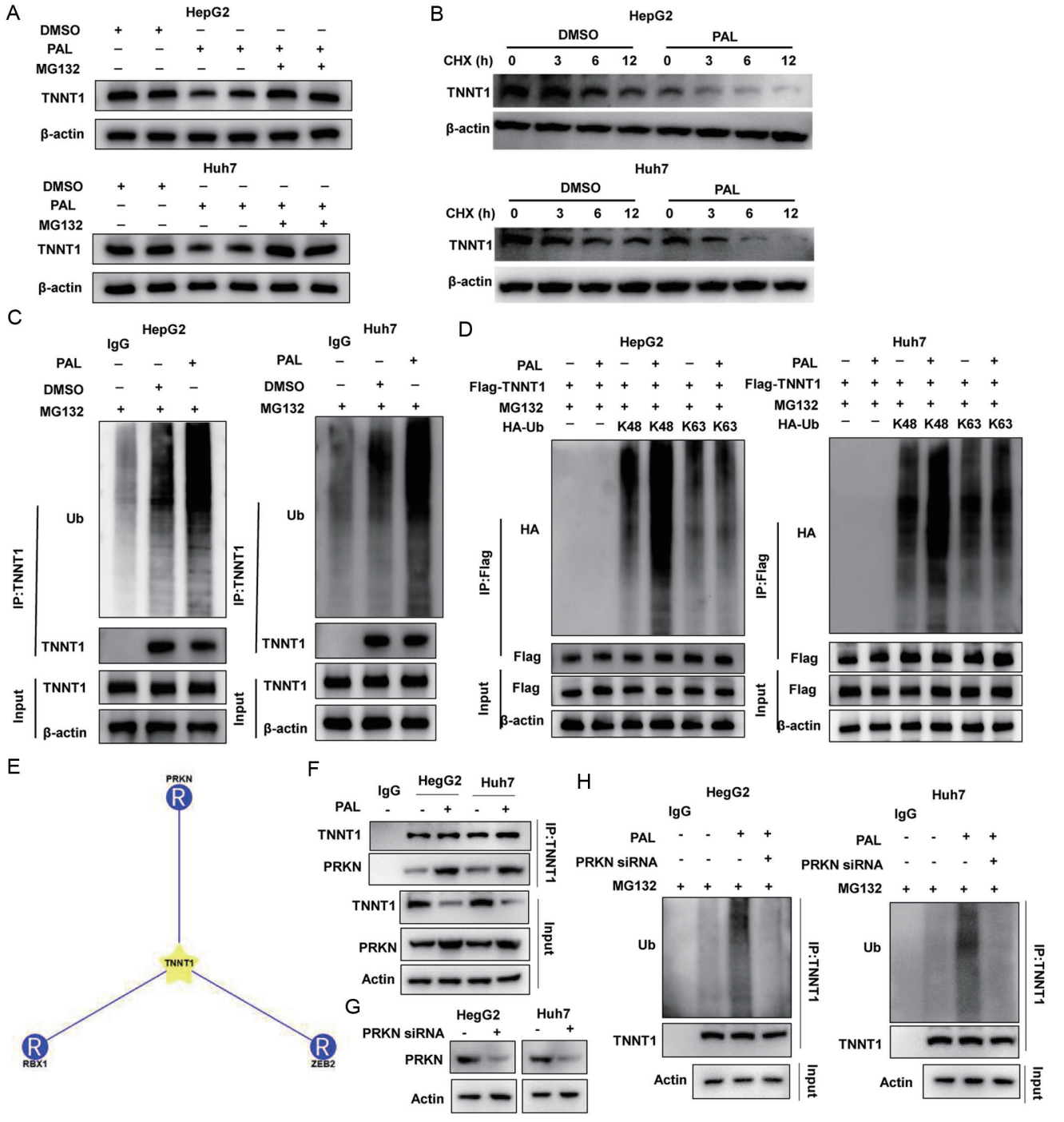

Fig. 4. The effects of PAL on K48-linked polyubiquitination and protein stability of TNNT1. (A) PAL-treated HCC cells Huh7 and HepG2 were treated with vehicle or the proteasome inhibitor MG132 (50 μM) for 3 h. Cell lysates were then blotted with the indicated antibodies. (B) CHX chase assays indicated the role of PAL in regulating the half-life of TNNT1 protein. (C) The role of PAL in TNNT1 ubiquitination. (D) The role of PAL in TNNT1 K48-linked and K63-linked polyubiquitination. (E) UbiBrowser 2.0 showing the potential E3 ligase for TNNT1 ubiquitination. (F) The effect of PAL on the interaction between exogenous PRKN and TNNT1. Cell lysates from PAL-treated Huh7 and HepG2 cells were subjected to immunoprecipitation with TNNT1 antibody and then blotted with the indicated antibodies. (G) HepG2 cells were transduced with PRKN siRNA pool, and cell lysates were blotted with the indicated antibodies. (H) The role of PRKN siRNA pool in PAL-mediated TNNT1 ubiquitination. HCC, hepatocellular carcinoma; PAL, palmatine; CHX, Cycloheximide; siRNA, small interfering RNA; TNNT1, troponin T1; DMSO, dimethyl sulfoxide; Ub, ubiquitin; IgG, Immunoglobulin G; PRKN, Parkinson disease protein 2; HA, human influenza hemagglutinin; +, with; -, without.

protein stability through the ubiquitin-proteasome system,[44] we next examined the effect of PAL on TNNT1 ubiquitination. As expected, treatment with PAL significantly increased the polyubiquitination of TNNT1 in both Huh7 and HepG2 cells compared with the Ctrl groups (Fig. 4C). To further characterize PAL-mediated TNNT1 ubiquitination, we performed ubiqui-

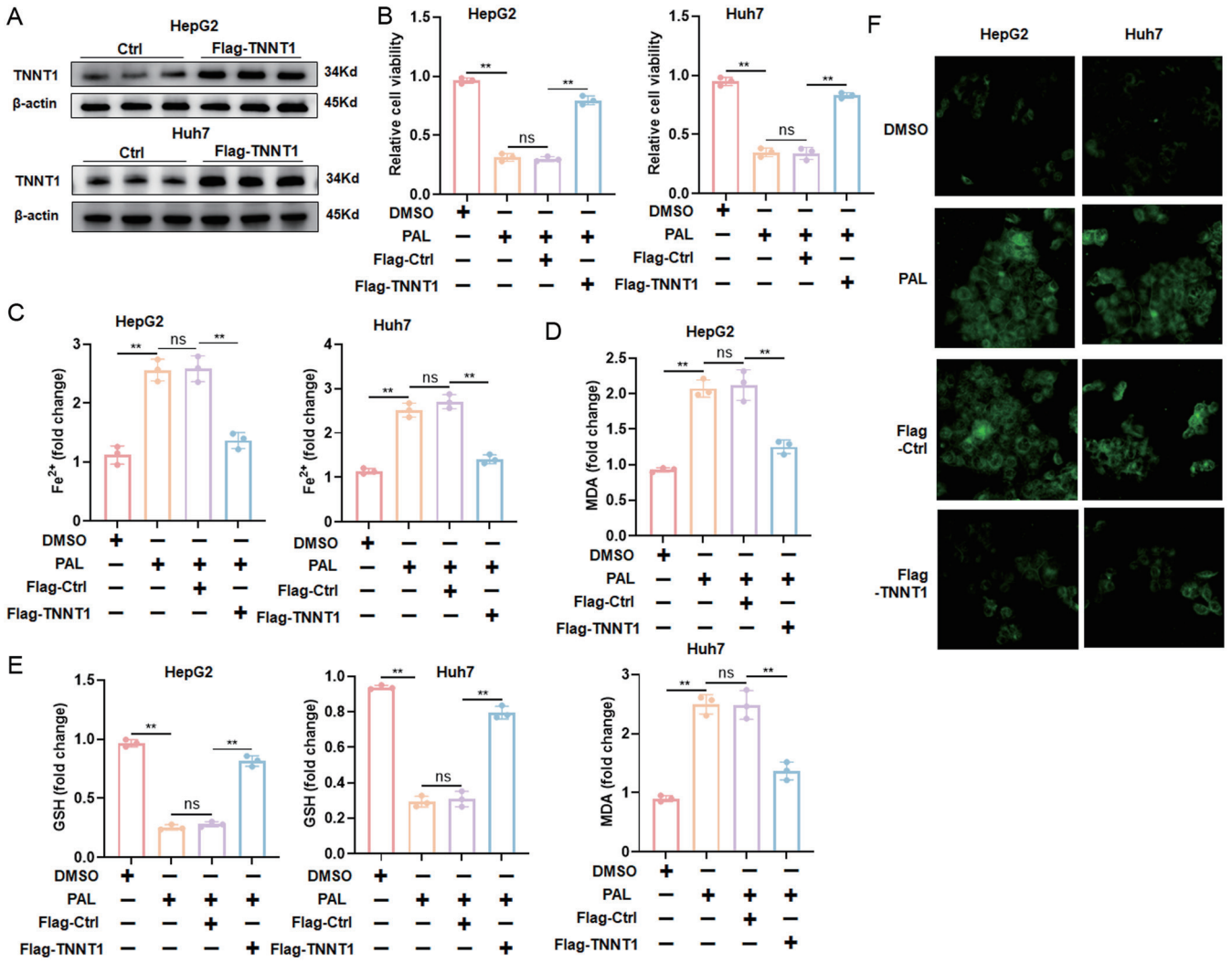

Fig. 5. Effects of TNNT1-dependent PAL activity on ferroptosis. (A) HCC cells Huh7 and HepG2 were transduced with Flag-TNNT1, and cell lysates were blotted with the indicated antibodies. (B) The CCK-8 assay indicated the regulatory effects of Flag-TNNT1 on PAL-mediated cell viability inhibition. (C) The regulatory effects of Flag-TNNT1 on the PAL-mediated increase in Fe^{2+}. (D) The regulatory effects of Flag-TNNT1 on the PAL-mediated increase in lipid peroxidation product MDA. (E) The regulatory effects of Flag-TNNT1 on the PAL-mediated decrease in GSH. (F) The regulatory effects of Flag-TNNT1 on the PAL-mediated increase in ROS. NS, not significant. **P* < 0.05;***P* < 0.01. HCC, hepatocellular carcinoma; CCK-8, Cell Counting Kit-8; PAL, palmatine; Fe^{2+}, ferrous iron; MDA, malondialdehyde; ROS, reactive oxygen species; GSH, reduced glutathione; TNNT1, troponin T1; DMSO, dimethyl sulfoxide; Ctrl, Control; +, with; -, without.

tin linkage-specific assays using a panel of ubiquitin mutants with only a single lysine residue preserved. We found that PAL treatment specifically enhanced K48-linked polyubiquitination of TNNT1 (Fig. 4D). Given the important roles of E3 ubiquitin ligases in protein ubiquitination,[45] we used UbiBrowser 2.0[46] to identify Parkinson disease protein 2 (PRKN) as the potential E3 ligase for TNNT1 ubiquitination (Fig. 4E). PAL treatment significantly enhanced the interaction between PRKN and TNNT1 (Fig. 4F). However, knockdown of PRKN abolished the stimulatory effects of PAL on TNNT1 ubiquitination in both Huh7 and HepG2 cells (Fig. 4G and H). Collectively, our data demonstrated that PAL promoted PRKN-mediated TNNT1 ubiquitination and degradation.

PAL participated in ferroptotic cell death through a TNNT1-dependent manner

To better characterize whether TNNT1 signaling affects PAL-mediated ferroptosis, we constructed a TNNT1 overexpression vector to restore TNNT1 protein levels (Fig. 5A). Interestingly, ectopic expression of TNNT1 in PAL-treated Huh7 and HepG2 cells completely reversed the decrease in cell viability (Fig. 5B). Next, we sought to confirm the anti-ferroptotic potential of TNNT1 against PAL. We used the Gene Expression Profiling Interactive Analysis 2 database[47] to examine the correlation between TNNT1 expression and ferroptosis-associated markers. As shown in Supplementary Figure 2A and B, a positive correlation between TNNT1 and several ferroptosis suppressors, such as ferritin heavy chain 1 (FTH1, $P = 0.012$, Pearson $r = 0.13$), heat shock protein beta-1 (HSPB1, $P = 7.5 \times 10^{-12}$, Pearson $r = 0.35$), and solute carrier family 7 member 11 (SLC7A11, $P = 0.049$, Pearson $r = 0.1$), was observed in human HCC specimens. TNNT1 expression also displayed a negative correlation with several ferroptosis drivers, such as lysophosphatidylcholine acyltransferase 3 (LPCAT3, $P = 0.054$, Pearson $r = -0.1$), nuclear receptor coactivator 4 (NCOA4, $P = 0.009$, Pearson

r = −0.14), and transferrin (TF, P = 0.0017, Pearson r = −0.16). These results indicated that TNNT1 might act as a negative regulator of ferroptosis. Notably, overexpression of TNNT1 effectively blocked the promoting effects of PAL on cellular Fe^{2+} and MDA levels (Fig. 5C and D). Meanwhile, the decreased GSH levels induced by PAL treatment were efficiently reversed by ectopic expression of TNNT1 in both Huh7 and HepG2 cells (Fig. 5E). Immunofluorescence staining showed that TNNT1 overexpression could also abolish PAL-mediated upregulation of cellular ROS concentrations (Fig. 5F). Therefore, these findings suggested that PAL generated ferroptotic cell death in a TNNT1-dependent manner.

The in vivo antitumor activity of PAL by regulating TNNT1

Previously, we demonstrated the pivotal functions of PAL in regulating ferroptosis, which were achieved by inhibiting TNNT1 levels. Next, we sought to validate these findings using BALB/c nude mouse xenograft models (Fig. 6A). Unsurprisingly, tumor size and weight were drastically suppressed after PAL monotherapy. However, TNNT1 overexpression diminished the antitumor effect of PAL (Fig. 6B–D). Meanwhile, western blot analysis of tumor tissue proteins showed decreased GPX4 and increased levels of the lipid peroxidation product 4-HNE following PAL treatment. However, TNNT1 overexpression distinctly antagonized these effects mediated by PAL (Fig. 6E). Next, we assessed whether PAL treatment or TNNT1 overexpression could cause adverse effects in mice. No significant changes in body weight were observed among groups during the experimental period (Fig. 6F). Given that alanine transaminase and aspartate transaminase reflect hepatic function, whereas creatinine indicates renal function, we measured their serum levels using spectrophotometry. No significant differences in serum alanine transaminase, aspartate transaminase, or creatinine levels were detected among the four groups (Fig. 6G). Furthermore, hematoxylin and eosin staining revealed no obvious histopathological abnormalities in several organs, including the heart, liver, spleen, lung, and kidney (Fig. 6H). Taken together, these results supported the potential clinical activity and negligible adverse effects of PAL against HCC.

Discussion

Nowadays, natural compounds represent promising bioactive agents owing to their distinct antitumor properties and minimal adverse effects.[48–50] Despite these merits, their detailed antitumor mechanisms are still poorly understood. Alkaloids, naturally occurring organic compounds, hold significant value in the clinical prevention and treatment of cancers, especially HCC.[51] The *Nelumbo nucifera*-derived alkaloid liensinine could impair glycolysis and the immunosuppressive microenvironment in HCC cells by activating the AMP-activated protein kinase-hypoxia-inducible factor-1α signaling axis, thereby enhancing therapeutic sensitivity.[52] Berberine, an isoquinoline alkaloid isolated from *Coptis chinensis*, significantly activates the anti-HCC immune response by enhancing the effector function of T lymphocytes.[53] In the present study, we used an alkaloid library to explore their underlying anti-HCC potential and identified the natural compound PAL as a promising candidate with remarkable anticancer activity. Moreover, *in vivo* models confirmed that PAL exhibited favorable clinical efficacy against HCC along with negligible adverse effects.

Accumulating evidence indicates that the induction of programmed cell death holds great promise for the development of novel antitumor therapies. As an iron-dependent form of programmed cell death, ferroptosis has rapidly become a hotspot with substantial scientific value and significant therapeutic potential.[54] In HCC cells, the highly bioactive alkaloid piperine displays pharmacological properties by eliciting ferroptotic cell death through increasing ROS activity and Fe^{2+} content.[55] Additionally, Li's group pointed out that berberine, a natural alkaloid from some medicinal herbs, induces ferroptosis in HepG2 cells by stimulating severe mitochondrial dysfunction and ROS accumulation.[56] Similarly, our work identified TNNT1 as the critical target for PAL-driven ferroptosis in HCC cells. The present study further clarified the mechanism by which TNNT1 inhibited ferroptosis. Correlation analysis using the Gene Expression Profiling Interactive Analysis 2 database showed that TNNT1 expression was positively correlated with multiple ferroptosis suppressors (e.g., FTH1, HSPB1, and SLC7A11), while being negatively correlated with ferroptosis drivers (e.g., TF, NCOA4, and LPCAT3) in human HCC tissues. These results suggest that TNNT1 might inhibit ferroptosis mainly through regulating iron metabolism, enhancing antioxidant capacity, and maintaining the SLC7A11/GPX4 signaling axis. Mechanistically, TNNT1 may reduce intracellular Fe^{2+} accumulation by upregulating FTH1 and downregulating TF, thereby limiting iron-dependent lipid peroxidation. Meanwhile, TNNT1 may elevate HSPB1 to alleviate oxidative stress and preserve GSH levels by enhancing SLC7A11-mediated cystine uptake, which further stabilizes GPX4 activity and inhibits ferroptosis. Consistently, functional rescue experiments confirmed that overexpression of TNNT1 significantly reversed PAL-induced increases in Fe^{2+}, MDA, and ROS, as well as the decrease in GSH.

Slow skeletal muscle TNNT1 acts as a poor prognostic biomarker in multiple human cancers, such as colon adenocarcinoma. Functional analyses suggested that increased TNNT1 could drive cellular malignant behaviors.[57] In lung cancer, knockdown of TNNT1 notably attenuates cell migration and invasion through suppressing the Wnt/β-catenin pathway.[58] Findings from Huang's group reported similar discoveries, confirming the oncogenic functions of TNNT1 in HCC.[37] Here, our findings also demonstrated that TNNT1 exerted a tumor-promoting role in HCC cells. Patients with high TNNT1 expression exhibited poor overall survival. Furthermore, overexpression of TNNT1 significantly antagonized both the tumor growth inhibition and ferroptosis induction mediated by PAL.

While this study clarifies that PAL promotes TNNT1 degradation to reverse ferroptosis resistance, several limitations need to be addressed. Specifically, only two HCC cell lines, Huh7 and HepG2, were employed to verify the biological effects of PAL on TNNT1 ubiquitination and ferroptosis induction. The applicability of these findings to other HCC cell subtypes (such as MHCC97H and SK-Hep-1) or primary HCC cells isolated from clinical samples remains unclear. Recently, ferroptosis has increasingly been recognized as a pivotal immunomodulatory mechanism that enhances anticancer immunity.[59] However, the *in vivo* experiments only adopted nude mouse xenograft models, which lack a functional immune system. This deficiency limits the assessment of potential crosstalk between PAL-induced TNNT1 degradation, ferroptosis activation, and remodeling of the tumor immune microenvironment. This study also failed to characterize the *in vivo* pharmacokinetic and pharmacodynamic profiles of PAL, including the optimal administration route and dosage in mouse models. Clarifying these pharmacokinetic/pharmacodynamic parameters is essential for facilitating the clinical translation of PAL as a potential anti-HCC therapeutic agent. In addition, whether other E3 ubiquitin ligases or deubiquitinating enzymes participate in TNNT1 stability warrants further exploration. Moreover, we mainly focused on TNNT1 as the primary downstream target of PAL. Whether other

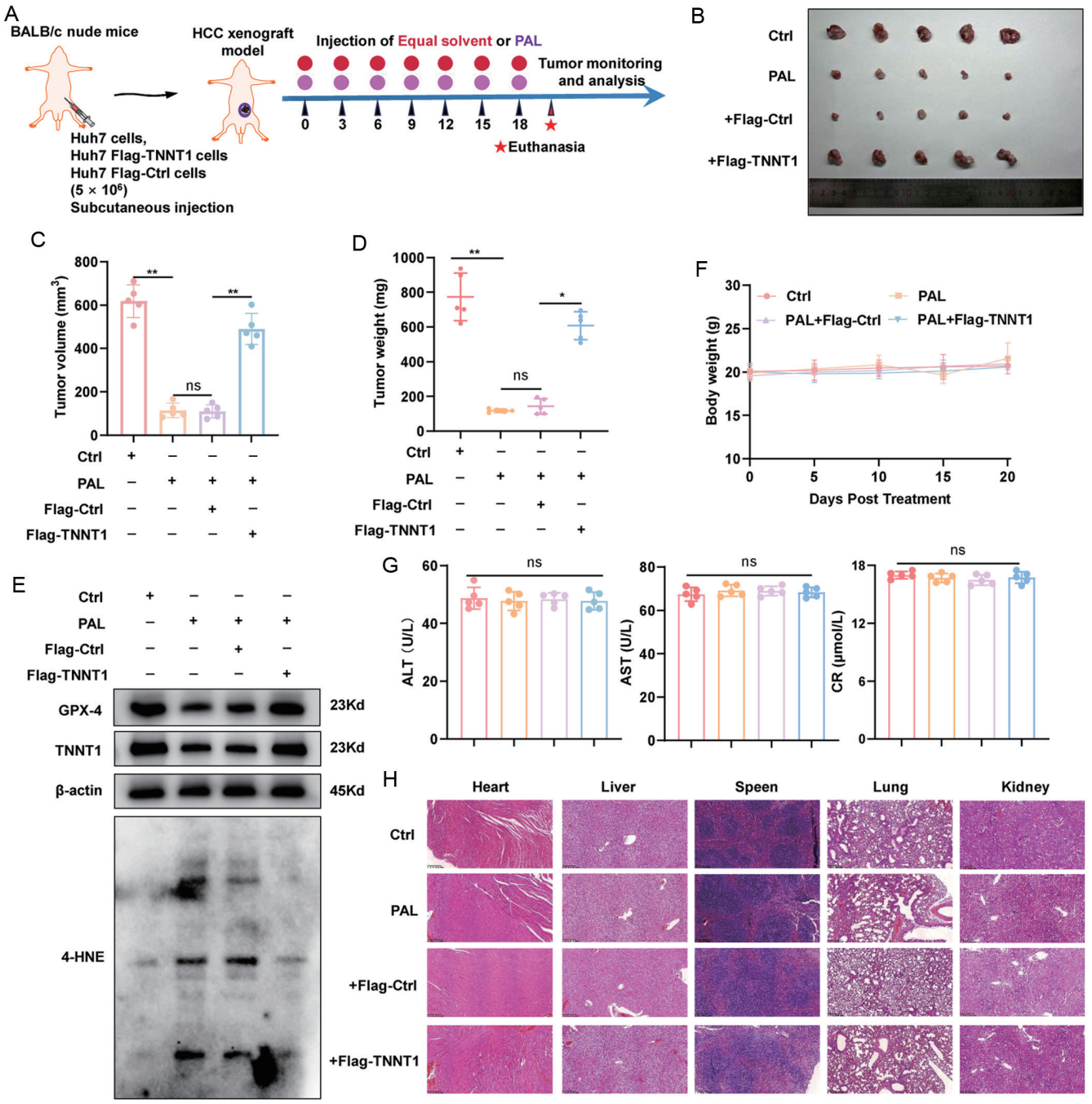

Fig. 6. ***In vivo*** **antitumor abilities of PAL against HCC.** (A) Schematic illustration of the experimental protocol for HCC xenograft models, which were treated with vehicle or PAL. (B) Representative photographs of tumors. (C-D) Quantitative analysis of tumor volume (C) and weight (D) in Huh7 xenograft-bearing mice following the indicated treatment. (E) Western blot analysis indicated the expression of GPX4, 4-HNE, and TNNT1 in tumor tissues. (F) Quantitative analysis of body weight in Huh7 xenograft-bearing mice following the indicated treatment. (G) The serum levels of ALT, AST, and CR. (H) H&E staining of several organs among the treated groups, including the heart, liver, spleen, lung, and kidney. NS, not significant. $^{**}P < 0.01$. HCC, hepatocellular carcinoma; H&E, hematoxylin and eosin; PAL, palmatine; ALT, alanine transaminase; AST, aspartate transaminase; CR, creatinine; TNNT1, troponin T1; GPX4, glutathione peroxidase 4; 4-HNE, 4-hydroxynonenal; Ctrl, Control; +, with; -, without.

downregulated proteins are target molecules of PAL requires further verification in future experiments.

Conclusions

We screened an alkaloid library and identified PAL as a candidate anti-HCC compound. Our work reveals that PAL reverses ferroptosis resistance by inducing TNNT1 ubiquitination and degradation. Using a combination of *in vitro* tumor cell experiments and *in vivo* xenograft models, we provide compelling evidence that PAL exerts its antitumor effect by inducing ubiquitination and subsequent degradation of TNNT1,

thereby restoring the sensitivity of HCC cells to ferroptosis. The clinical significance of this study lies in identifying a novel anti-HCC strategy and providing new insights into targeted therapy for HCC. PAL, a bioactive natural alkaloid with potent antitumor properties, promotes ferroptosis through TNNT1 downregulation. Our discovery demonstrates the promising prospects of PAL for anti-HCC clinical translation and provides a novel therapeutic target and treatment paradigm. Notably, PAL displays a satisfactory safety profile, laying a solid foundation for its future clinical application. Its unique mechanism also fills a gap in current HCC treatment and provides a new option for patients lacking effective therapies.

Supporting information

Supplementary material for this article is available at https://doi.org/10.14218/JCTH.2026.00215.

Funding

This study was supported by grants from the Natural Science Foundation of Hunan Province of China (2025JJ80099), the Natural Science Foundation of Changsha (kq2403032), the Guangdong Basic and Applied Basic Research Foundation (2023A1515111116), and the Shenzhen Foundation of Science and Technology (JCYJ20230807151308018).

Conflict of interest

The authors have no conflict of interests related to this publication.

Author contributions

Study design (XW, ZX), writing of the original draft (ZZ), review of the manuscript (FX, CW, SZ, JW). All authors contributed to the article and approved the submitted version.

Ethical statement

The mouse experiments were conducted in accordance with relevant institutional guidelines for animal care and use, and approved by the Ethics Committee of Xiangya Hospital, Central South University (Approval Number: XY20260303003). All animals received humane care.

Data sharing statement

The data analyzed during the current study are available from the corresponding author upon reasonable request.

References

[1] Liu J, Lv Y, Liu K, Li Z, Chen B, Bu Y. MED10 as a Novel Oncogenic Driver in HCC: Promoting Cell Cycle Progression and Proliferation Through RAF1 Activation. Front Biosci (Landmark Ed) 2025;30(8):39944. doi:10.31083/FBL39944, PMID:40917057.

[2] Cao M, Cao M, Xia C, Yang F, Yan X, He S, *et al*. Score-based prediction model for female hepatocellular carcinoma surveillance in asymptotic HBsAg carriers: a multicenter cohort study in China. J Natl Cancer Cent 2025;5(5):493–500. doi:10.1016/j.jncc.2025.05.005, PMID:41111927.

[3] Pinter M, Iavarone M. Reversing the global burden of hepatocellular carcinoma. J Hepatol 2026;84(5):853–854. doi:10.1016/j.jhep.2026.01.017, PMID:41638493.

[4] Nooreen Z, Wal A, Shukla A, Badarinath AV, Kumar N, Sarma T, *et al*. Emerging DNA- and RNA-based therapeutic strategies in hepatocellular carcinoma: A molecular approach to precision medicine. Lett Drug Des Discov 2025;22(11):100268. doi:10.1016/j.lddd.2025.100268.

[5] Gudivada IP, Amajala KC. Integrative Bioinformatics Analysis for Targeting Hub Genes in Hepatocellular Carcinoma Treatment. Curr Genomics 2025;26(1):48–80. doi:10.2174/0113892029308243240709073945, PMID:39911278.

[6] Sensi B, Angelico R, Toti L, Conte L, Coppola A, Tisone G, *et al*. Mechanism, Potential, and Concerns of Immunotherapy for Hepatocellular Carcinoma and Liver Transplantation. Curr Mol Pharmacol 2024;17:e18761429310703. doi:10.2174/0118761429310703240823045808, PMID:39225204.

[7] Tan Z, Chen Y, Peng Y, Tang Y, Sun B, Zhou J, *et al*. Integration of Meta-Analysis and Network Pharmacology to Investigate the Pharmacological Mechanisms of Quercetin on Hepatocellular Carcinoma. Front Biosci (Landmark Ed) 2025;30(11):46289. doi:10.31083/FBL46289, PMID:41351405.

[8] Ge G, Jiang X, Tian X, Zhou Y, Cao G. The role of Salvia miltiorrhiza compounds in hepatocellular carcinoma: a preliminary investigation based on computational analysis and liquid chromatography-tandem mass spectrometry. Curr Pharm Anal 2025;21(4):249–264. doi:10.1016/j.cpan.2025.04.001.

[9] Yamada T, Tateishi R, Fujishiro M. Post-transplant hepatocellular carcinoma: balancing immunosuppression and immune checkpoint inhibitors. Clin Mol Hepatol 2026;32(2):580–598. doi:10.3350/cmh.2025.1179, PMID:41622628.

[10] Li J, Huang Y, Li J, Shi M, Xiao Y, Du F, *et al*. Metabolic reprogramming-driven resistance to multi-kinase inhibitors in hepatocellular carcinoma: molecular mechanisms and therapeutic opportunities. Mol Cancer 2026;25(1):37. doi:10.1186/s12943-026-02578-w, PMID:41593671.

[11] An L, Li Z. Molecular network of metabolic reprogramming and precision diagnosis and treatment of hepatocellular carcinoma. Biomark Res 2025;13(1):124. doi:10.1186/s40364-025-00844-5, PMID:41074146.

[12] Elmetwalli A. Ferroptosis and the cGAS-STING pathway into precision nano-immuno-theranostics: A mechanistic paradigm for reversing drug resistance in hepatocellular carcinoma. Drug Resist Updat 2026;84:101326. doi:10.1016/j.drup.2025.101326, PMID:41275854.

[13] Dai X, Zheng Y, Cui J, Zeng Y, Yang B, Zhang Z. Nanodrug delivery systems targeting ferroptosis as an innovative therapeutic approach for Rheumatoid Arthritis. Mater Today Bio 2025;32:101804. doi:10.1016/j.mtbio.2025.101804, PMID:40343168.

[14] Gao Y, Xu J, Lai Y, Fan Y, Zhou Y, Tu Y, *et al*. 2D nanomaterial-triggered ferroptosis in cancer therapy. J Nanobiotechnology 2025;24(1):81. doi:10.1186/s12951-025-03975-x, PMID:41449419.

[15] Yang Z, Tai Y, Lan T, Zhao C, Gao JH, Tang CW, *et al*. Inhibition of Cyclooxygenase-2 Upregulates the Nuclear Factor Erythroid 2-related Factor 2 Signaling Pathway to Mitigate Hepatocyte Ferroptosis in Chronic Liver Injury. J Clin Transl Hepatol 2025;13(5):409–417. doi:10.14218/JCTH.2024.00440, PMID:40385941.

[16] Luo R, Li S, Wang H, Zhang Z, Li L, Shang P. Thymoquinone suppresses cell growth and induces ferroptosis in renal cell carcinoma by reducing SERPINH1 expression. Lett Drug Des Discov 2025;22(2):100013. doi:10.1016/j.lddd.2025.100013.

[17] Wang J, Chen Z, Liu W, Xu Z, Liu H, Li Y, *et al*. Harnessing plant-derived natural compounds to target ferroptosis, pyroptosis, immune modulation and renin-angiotensin system in renal cell carcinoma. J Renin Angiotensin Aldosterone Syst 2025;26:1–18. doi:10.1177/14703203251386309.

[18] Meng Y, Chen Q, Zhou Z, Li M. Regulated cell death in cancer: Mechanisms, crosstalk, and opportunities for therapy. Cancer Lett 2025;635:218077. doi:10.1016/j.canlet.2025.218077, PMID:41130559.

[19] Chen L, Li H, Luo Q, Zhou H, Song H, Liu X, *et al*. G6PD(+)CSV(+) circulating tumor cells associated with portal vein tumor thrombus formation via EMT-ferroptosis crosstalk: a dual biomarker for therapeutic efficacy and prognosis prediction in hepatocellular carcinoma. Cancer Lett 2026;639:218205. doi:10.1016/j.canlet.2025.218205, PMID:41352523.

[20] Tao Y, Yin S, Wei K, Zhao L, Cui Y, Li C, *et al*. SCRN1 confers hepatocellular carcinoma resistance to ferroptosis by stabilizing GPX4 via STK38-mediated phosphorylation. Nat Cancer 2025;6(12):1976–1993. doi:10.1038/s43018-025-01061-7, PMID:41145774.

[21] Yan Y, Hu J, Han N, Li HT, Yang X, Li LG, *et al*. Sorafenib-loaded metal-organic framework nanoparticles for anti-hepatocellular carcinoma effects through synergistically potentiating ferroptosis and remodeling tumor immune microenvironment. Mater Today Bio 2025;32:101848. doi:10.1016/j.mtbio.2025.101848, PMID:40487165.

[22] Fan H, Wang C, Liu S, Li Y, Xu Z. Therapeutic potential of natural products in stress granules: Underlying molecular mechanisms and future perspectives. Curr Pharm Anal 2025;21(2):88–99. doi:10.1016/j.cpan.2025.01.004.

[23] Yan Y, Su W, Zeng S, Qian L, Chen X, Wei J, *et al*. Effect and Mechanism of Tanshinone I on the Radiosensitivity of Lung Cancer Cells. Mol Pharm 2018;15(11):4843–4853. doi:10.1021/acs.molpharmaceut.8b00489, PMID:30216081.

[24] Guo L, Zhao W, Wang H, Qiu S, Wang R, Zhang J, *et al*. Mechanisms of Traditional Chinese Medicine-Derived Alkaloids in Colorectal Cancer Therapy: Molecular Targets, Preclinical Evidence, and Translational Prospects. Drug Des Devel Ther 2026;20:564320. doi:10.2147/DDDT.S564320, PMID:42261447.

[25] Sun D, Hua Z, Xiao Y, He D, Wu H, Lin X, *et al*. Bidirectional microbial regulation by tyrosine metabolism enhances palmatine-mediated colitis protection. Gut Microbes 2025;17(1):2596405. doi:10.1080/19490976.2025.2596405, PMID:41362927.

[26] Chakravarthy D, Muñoz AR, Su A, Hwang RF, Keppler BR, Chan DE, *et al*. Palmatine suppresses glutamine-mediated interaction between pancreatic cancer and stellate cells through simultaneous inhibition of survivin and COL1A1. Cancer Lett 2018;419:103–115. doi:10.1016/j.canlet.2018.01.057, PMID:29414301.

[27] Tang W, Li J, Zhou Y, Li J, Ma Z, Li X, *et al*. Palmatine attenuates MYH9 mediated nuclear localization of AURKA to induce G2/M phase arrest in colorectal cancer cells. Int Immunopharmacol 2024;143(Pt 3):113615. doi:10.1016/j.intimp.2024.113615, PMID:39536490.

[28] Ativui S, Danquah CA, Ossei PPS, Ofori M. Palmatine Attenuates Metastatic Lung Colonization of Triple Negative Breast Cancer Cells. Front Pharmacol 2022;13:853230. doi:10.3389/fphar.2022.853230, PMID:35496301.
[29] Chen J, Wang T, Xu S, Lin A, Yao H, Xie W, *et al*. Design, synthesis and biological evaluation of novel nitric oxide-donating protoberberine derivatives as antitumor agents. Eur J Med Chem 2017;132:173–183. doi:10.1016/j.ejmech.2017.03.027, PMID:28359045.
[30] Lu J, Tang M, Li H, Xu Z, Weng X, Li J, *et al*. EBV-LMP1 suppresses the DNA damage response through DNA-PK/AMPK signaling to promote radioresistance in nasopharyngeal carcinoma. Cancer Lett 2016;380(1):191–200. doi:10.1016/j.canlet.2016.05.032, PMID:27255972.
[31] Zhou S, Zhu X, Xu Z, Yi Q, Wang J, Wang X, *et al*. Gramine suppresses triple-negative breast cancer by inducing ferroptosis via CUL3-mediated ubiquitination of MTDH. Curr Mol Pharmacol 2026;19(1):14–26. doi:10.1016/j.cmp.2026.03.001.
[32] Bian Y, Shan G, Bi G, Xu Z, Liang J, Yan Y, *et al*. Targeting polyamine metabolism and ferroptosis enhances the efficacy of KRAS-targeted therapy depending on KEAP1 status. Nat Commun 2025;16(1):9923. doi:10.1038/s41467-025-65441-4, PMID:41219185.
[33] Bao Y, Li G, Li S, Zhou H, Yang Z, Wang Z, *et al*. A novel nanomedicine integrating ferroptosis and photothermal therapy, well-suitable for PD-L1-mediated immune checkpoint blockade. Mater Today Bio 2024;29:101346. doi:10.1016/j.mtbio.2024.101346, PMID:39635320.
[34] Liu J, Tang D, Kang R. Targeting GPX4 in ferroptosis and cancer: chemical strategies and challenges. Trends Pharmacol Sci 2024;45(8):666–670. doi:10.1016/j.tips.2024.05.006, PMID:38866667.
[35] Chen R, Zou J, Liu J, Kang R, Tang D. DAMPs in the immunogenicity of cell death. Mol Cell 2025;85(20):3874–3889. doi:10.1016/j.molcel.2025.09.007, PMID:41106375.
[36] Jafari R, Almqvist H, Axelsson H, Ignatushchenko M, Lundbäck T, Nordlund P, *et al*. The cellular thermal shift assay for evaluating drug target interactions in cells. Nat Protoc 2014;9(9):2100–2122. doi:10.1038/nprot.2014.138, PMID:25101824.
[37] Huang SC, Huang CC, Ko CY, Huang CY, Liu CH, Lee YK, *et al*. Slow skeletal muscle troponin T acts as a potential prognostic biomarker and therapeutic target for hepatocellular carcinoma. Gene 2023;865:147331. doi:10.1016/j.gene.2023.147331, PMID:36871674.
[38] Jiang Z, Wu Y, Miao Y, Deng K, Yang F, Xu S, *et al*. HCCDB v2.0: Decompose Expression Variations by Single-cell RNA-seq and Spatial Transcriptomics in HCC. Genomics Proteomics Bioinformatics 2024;22(1):qzae011. doi:10.1093/gpbjnl/qzae011, PMID:38886186.
[39] Győrffy B. Integrated analysis of public datasets for the discovery and validation of survival-associated genes in solid tumors. Innovation (Camb) 2024;5(3):100625. doi:10.1016/j.xinn.2024.100625, PMID:38706955.
[40] Grinchuk OV, Yenamandra SP, Iyer R, Singh M, Lee HK, Lim KH, *et al*. Tumor-adjacent tissue co-expression profile analysis reveals pro-oncogenic ribosomal gene signature for prognosis of resectable hepatocellular carcinoma. Mol Oncol 2018;12(1):89–113. doi:10.1002/1878-0261.12153, PMID:29117471.
[41] Hoshida Y, Nijman SM, Kobayashi M, Chan JA, Brunet JP, Chiang DY, *et al*. Integrative transcriptome analysis reveals common molecular subclasses of human hepatocellular carcinoma. Cancer Res 2009;69(18):7385–7392. doi:10.1158/0008-5472.CAN-09-1089, PMID:19723656.
[42] Lin A, Yang H, Shi Y, Li K, Chen L, Wong HZH, *et al*. PanCanSurvPlot: A large-scale pan-cancer survival analysis web application. Curr Proteomics 2025;22(6):100062. doi:10.1016/j.curpro.2025.100062.
[43] Yan Y, Xu Z, Huang J, Guo G, Gao M, Kim W, *et al*. The deubiquitinase USP36 Regulates DNA replication stress and confers therapeutic resistance through PrimPol stabilization. Nucleic Acids Res 2020;48(22):12711–12726. doi:10.1093/nar/gkaa1090, PMID:33237263.
[44] Song S, Hua S, Chen G, Yin X, Chen Z, Li C, *et al*. Identification of Pinostilbene as a natural STING agonist that triggers FTH1 degradation via K48-ubiquitination to induce ferroptosis in non-small cell lung cancer. Redox Biol 2026;91:104099. doi:10.1016/j.redox.2026.104099, PMID:41723905.
[45] Zhang N, Yang P, Li Y, Ouyang Q, Hou F, Zhu G, *et al*. Serum Iron Overload Activates the SMAD Pathway and Hepcidin Expression of Hepatocytes via SMURF1. J Clin Transl Hepatol 2024;12(3):227–235. doi:10.14218/JCTH.2023.00440, PMID:38426189.
[46] Wang X, Li Y, He M, Kong X, Jiang P, Liu X, *et al*. UbiBrowser 2.0: a comprehensive resource for proteome-wide known and predicted ubiquitin ligase/deubiquitinase-substrate interactions in eukaryotic species. Nucleic Acids Res 2022;50(D1):D719–D728. doi:10.1093/nar/gkab962, PMID:34669962.
[47] Tang Z, Kang B, Li C, Chen T, Zhang Z. GEPIA2: an enhanced web server for large-scale expression profiling and interactive analysis. Nucleic Acids Res 2019;47(W1):W556–W560. doi:10.1093/nar/gkz430, PMID:31114875.
[48] Yan Y, Yang X, Han N, Liu Y, Liang Q, Li LG, *et al*. Metal-organic framework-encapsulated dihydroartemisinin nanoparticles induces apoptotic cell death in ovarian cancer by blocking ROMO1-mediated ROS production. J Nanobiotechnology 2023;21(1):204. doi:10.1186/s12951-023-01959-3, PMID:37386404.
[49] Wu G, Yan Y, Zhou Y, Duan Y, Zeng S, Wang X, *et al*. Sulforaphane: Expected to Become a Novel Antitumor Compound. Oncol Res 2020;28(4):439–446. doi:10.3727/096504020X15828892654385, PMID:32111265.
[50] Wei J, Yan Y, Chen X, Qian L, Zeng S, Li Z, *et al*. The Roles of Plant-Derived Triptolide on Non-Small Cell Lung Cancer. Oncol Res 2019;27(7):849–858. doi:10.3727/096504018X15447833065047, PMID:30982492.
[51] Qian R, Ge J, Fan N, Sun Z, Zhao C, Sun Y, *et al*. Natural Products in Cancer Prevention and Therapy: Current Challenges and Future Directions. MedComm (2020) 2026;7(2):e70585. doi:10.1002/mco2.70585, PMID:41614206.
[52] Liu J, Zhang X, Fan X, Liu P, Mi Z, Tan H, *et al*. Liensinine reshapes the immune microenvironment and enhances immunotherapy by reprogramming metabolism through the AMPK-HIF-1α axis in hepatocellular carcinoma. J Exp Clin Cancer Res 2025;44(1):208. doi:10.1186/s13046-025-03477-6, PMID:40665352.
[53] Hu J, Shi Q, Xue C, Wang Q. Berberine Protects against Hepatocellular Carcinoma Progression by Regulating Intrahepatic T Cell Heterogeneity. Adv Sci (Weinh) 2024;11(39):e2405182. doi:10.1002/advs.202405182, PMID:39135526.
[54] Kang R, Liu J, Wang J, Kroemer G, Tang D. Translating ferroptosis into oncology: challenges, opportunities and future directions. Nat Rev Clin Oncol 2026;23(6):401–424. doi:10.1038/s41571-026-01128-z, PMID:41735603.
[55] Degirmenci NS, Yildirim Z, Padar G, Sahin F, Omeroglu Ulu Z. Combination of sodium pentaborate pentahydrate, curcumin and piperine treatment induces ferroptosis in hepatocellular carcinoma cells by regulating iron homeostasis and ROS activity in vitro. Med Oncol 2026;43(3):129. doi:10.1007/s12032-025-03223-0, PMID:41642374.
[56] Li K, Yi X, Yu Z, Xue K, Wu Y, Zhao Y, *et al*. Berberine sensitizes liver cancer cells to sorafenib by inducing SETDB1/NQO1/p53-dependent ferroptosis and genomic instability. Eur J Pharmacol 2025;1007:178211. doi:10.1016/j.ejphar.2025.178211, PMID:41082996.
[57] Hao YH, Yu SY, Tu RS, Cai YQ. TNNT1, a prognostic indicator in colon adenocarcinoma, regulates cell behaviors and mediates EMT process. Biosci Biotechnol Biochem 2020;84(1):111–117. doi:10.1080/09168451.2019.1664891, PMID:31512553.
[58] Ge X, Du G, Zhou Q, Yan B, Yue G. TNNT1 accelerates migration, invasion and EMT progression in lung cancer cells. Thorac Cancer 2024;15(23):1749–1756. doi:10.1111/1759-7714.15400, PMID:38973201.
[59] Bell HN, Stockwell BR, Zou W. Ironing out the role of ferroptosis in immunity. Immunity 2024;57(5):941–956. doi:10.1016/j.immuni.2024.03.019, PMID:38749397.